

## 4,4'-Dipyridylamine-Bridged Binuclear Complexes of Pentacyanoferrate and Pentaammineruthenium

Ching-Lung Lin, Kenneth Hung, and Andrew Yeh\*

Department of Chemistry, Tunghai Christian University,  
Taichung, Taiwan, Republic of China

Hsiu-Tun Tsen and Chan-Cheng Su

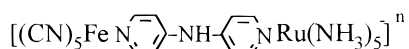
Department of Chemistry, National Taiwan Normal  
University, Taipei, Taiwan, Republic of China

Received January 27, 1998

### Introduction

In recent years there have been numerous studies on the binuclear complexes of pentacyanoferrate(II,III) and pentaammineruthenium(II,III).<sup>1–6</sup> In addition to the investigations in the spectral and electrochemical aspects which are usually emphasized in the mixed-valence chemistry of the diruthenium system,<sup>7</sup> the research works of this system have been extended to the study of the reactivity of the mixed valence compounds.<sup>2,5,6</sup> Nevertheless, most of the previous works in the characterization of the binuclear complexes of this kind were focused on both the reduced form and the mixed valence species; and little effort has been devoted to the investigation of the oxidized form. One of the reasons may be the difficulty in the detection of the species due to the lack of the spectral characteristics. Moreover, none of the binuclear complex (CN)<sub>5</sub>Fe<sup>III</sup>LRu<sup>III</sup>(NH<sub>3</sub>)<sub>5</sub> has ever been isolated.

In the study of the mixed valence chemistry of diruthenium binuclear complex with 4,4'-dipyridylamine as the bridging ligand,<sup>8</sup> it was found that the oxidized species Ru<sup>III</sup>-L-Ru<sup>III</sup> is characterized by a strong absorption in the visible region ( $\lambda_{\max} = 505$  nm,  $\log \epsilon = 3.74$ ) due to the  $\pi \rightarrow d\pi$  transition originating from the nitrogen lone pair electrons of the amine linkage in the bridging ligand.<sup>9</sup> Taking advantage of the strong LMCT absorption for this ligand, we undertook the investigation of the binuclear complexes



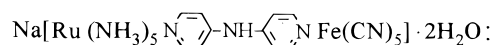
( $n = -1, 0, +1$ ), in the hope that the results may also help understand the properties and stability of the oxidized form of the binuclear complex.

### Experimental Section

**Materials.** Chloropentaammineruthenium(III) chloride,<sup>10</sup> sodium aminopentacyanoferrate(II)trihydrate,<sup>11,12</sup> and 4,4'-dipyridylamine<sup>8,13</sup> were prepared according to cited literature methods. [Ru(NH<sub>3</sub>)<sub>5</sub>-

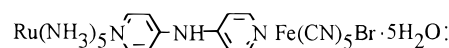
pyNHpyH](PF<sub>6</sub>)<sub>3</sub> and [Ru(NH<sub>3</sub>)<sub>5</sub>pyNHpyH]Br<sub>4</sub>·H<sub>2</sub>O were synthesized by the methods described by Sutton<sup>8</sup> except that the complexes were precipitated with different salts. A solution of (CN)<sub>5</sub>FepyNHpyRu(NH<sub>3</sub>)<sub>5</sub><sup>-</sup> (**R**) was prepared by mixing Fe(CN)<sub>5</sub>OH<sub>2</sub><sup>3-</sup> ( $\sim 1 \times 10^{-5}$  M) with an equimolar amount of Ru(NH<sub>3</sub>)<sub>5</sub>L<sup>2+</sup> at pH = 8 (tris). Solutions of (CN)<sub>5</sub>FepyNHpyRu(NH<sub>3</sub>)<sub>5</sub>(**M**) and [(CN)<sub>5</sub>FeLRu(NH<sub>3</sub>)<sub>5</sub>]<sup>+</sup> (**O**) were prepared by the oxidation of R with 1 and 2 equiv of S<sub>2</sub>O<sub>8</sub><sup>2-</sup>, respectively. All other chemicals were of reagent grade and were used as received.

**Synthesis of Binuclear Complexes.** Na[(CN)<sub>5</sub>FepyNHpyRu(NH<sub>3</sub>)<sub>5</sub>]·2H<sub>2</sub>O. A 9.6 mg amount of Na<sub>3</sub>[Fe(CN)<sub>5</sub>]·3H<sub>2</sub>O was added to 10 mL of a pre-deaerated solution containing an equimolar amount of [Ru(NH<sub>3</sub>)<sub>5</sub>pyNHpyH](PF<sub>6</sub>)<sub>3</sub>. The resulting solution was bubbled with argon for 20 min. After cooling in an ice bath for 30 min under argon atmosphere, the precipitate that formed was filtered out and washed with ethanol and ether. Yield: 7.8 mg. Anal. Calcd for



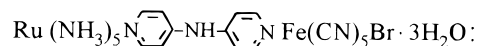
C, 29.9; N, 30.2; H, 4.68. Found: C, 29.5; N, 30.1; H, 4.39.

(CN)<sub>5</sub>FepyNHpyRu(NH<sub>3</sub>)<sub>5</sub>·5H<sub>2</sub>O. A pre-deaerated solution (10 mL) of  $1.0 \times 10^{-4}$  M (CN)<sub>5</sub>FepyNHpyRu(NH<sub>3</sub>)<sub>5</sub><sup>-</sup> was treated with 1 equiv of Na<sub>2</sub>S<sub>2</sub>O<sub>8</sub> under argon. The reaction was allowed to proceed for 10 min. The solution then was cooled to 0 °C. The resulting solid was filtered out and washed with ethanol and ether. Yield: 9.5 mg. Anal. Calcd for



C, 28.5; N, 28.8; H, 5.41. Found: C, 28.6; N, 28.9; H, 5.32.

[(CN)<sub>5</sub>FepyNHpyRu(NH<sub>3</sub>)<sub>5</sub>]Br·3H<sub>2</sub>O. A 100 mL pre-deaerated solution containing  $5.0 \times 10^{-4}$  M Fe(CN)<sub>5</sub>OH<sub>2</sub><sup>3-</sup> (prepared by aequation of Fe(CN)<sub>5</sub>NH<sub>3</sub><sup>3-</sup>) was transferred to 25 mL of a solution containing 36 mg [Ru(NH<sub>3</sub>)<sub>5</sub>pyNHpyH]Br<sub>4</sub>·H<sub>2</sub>O under argon atmosphere. A 1.2 equiv amount of Na<sub>2</sub>S<sub>2</sub>O<sub>8</sub> then was added, and the solution was kept bubbling with argon for another 2 min. After the solution cooled in an ice bath for 10 min, the precipitate that formed was filtered out and washed with ice-water, ethanol, and ether. Yield: 12 mg. Anal. Calcd for



C, 26.6; N, 26.9; H, 4.46. Found: C, 26.8; N, 26.9; H, 4.14.

**Kinetic Measurements.** Rates of formation of Fe(CN)<sub>5</sub>L<sup>3-</sup> complexes were measured by mixing freshly prepared Fe(CN)<sub>5</sub>OH<sub>2</sub><sup>3-</sup> solutions with excess ligands. Rates of dissociation of the corresponding Fe(II) complexes were measured by adding an excess amount of *N*-methylpyrazinium<sup>14</sup> to the solutions and following the formation of the Fe(CN)<sub>5</sub>spzCH<sub>3</sub><sup>3+</sup> complex at its band maximum (655 nm). The kinetics of the oxidation of Fe(II) and Ru(II) mono- and binuclear complexes by S<sub>2</sub>O<sub>8</sub><sup>2-</sup> were investigated by following the absorption decrease at  $\lambda_{\max}$  of the corresponding M(II) (M = Fe, Ru) complexes. All kinetic runs were carried out either on a photol RA401 stopped-flow apparatus or on a Hitachi U-2000 spectrophotometer. The observed rate constants were obtained from the slopes of linear least-square fits of  $\ln(A_{\infty} - A_t)$  vs time plots.

### Results and Discussion

**Characterization of the Mixed Valence Molecule.** The characteristic MLCT and LMCT spectra of the binuclear

- (1) Yeh, A.; Haim, A. *J. Am. Chem. Soc.* **1985**, *107*, 369.
- (2) Burewicz, A.; Haim, A. *Inorg. Chem.* **1988**, *27*, 1611.
- (3) Olabe, J. A.; Haim, A. *Inorg. Chem.* **1989**, *28*, 3277.
- (4) Huang, H. Y.; Chen, W. J.; Yang, C. C.; Yeh, A. *Inorg. Chem.* **1991**, *30*, 1862.
- (5) Parise, A. P.; Baraldo, L. M.; Olabe, J. A. *Inorg. Chem.* **1996**, *35*, 5080.
- (6) Almaraz, A. E.; Gentil, L. A.; Baraldo, L. M.; Olabe, J. A. *Inorg. Chem.* **1996**, *35*, 7718.
- (7) Creutz, C.; Prog. *Inorg. Chem.* **1983**, *30*, 1.
- (8) Sutton, J. E.; Taube, H. *Inorg. Chem.* **1981**, *20*, 3125.
- (9) Sutton, J. E.; Taube, H. *Inorg. Chem.* **1981**, *20*, 4021.
- (10) Vogt, L. H.; Katz, J. L.; Wiberly, S. E. *Inorg. Chem.* **1965**, *4*, 1158.

- (11) Brauer, G. *Handbook of Preparative Inorganic Chemistry*, 2nd ed.; Academic Press: New York, 1965; Vol. 2, p 1511.
- (12) Jwo, J. J.; Haim, A. *J. Am. Chem. Soc.* **1976**, *98*, 1172.
- (13) Koenigs, E.; Jung, G. *J. Prakt. Chem.* **1933**, *137*, 145.
- (14) Bahner, C. T.; Norton, L. L. *J. Am. Chem. Soc.* **1950**, *72*, 2881.

**Table 1.** Absorption Spectra of Iron(II,III) and Ruthenium(II,III) Complexes<sup>a</sup>

Complex	$\lambda_{\max}$ , nm	$10^{-3} \epsilon_{\max}$ , M <sup>-1</sup> cm <sup>-1</sup>	$\nu_{\text{CN}}$ , cm <sup>-1</sup>	$\delta(\text{NH}_3)_{\text{sym}}$ , cm <sup>-1</sup>
$\text{Fe}(\text{CN})_5 \text{N} \begin{array}{c} \diagup \diagdown \\ \diagdown \diagup \end{array} \text{NH} \begin{array}{c} \diagup \diagdown \\ \diagdown \diagup \end{array} \text{N}^{3-}$	368	7.19		
$\text{Fe}(\text{CN})_5 \text{N} \begin{array}{c} \diagup \diagdown \\ \diagdown \diagup \end{array} \text{NH} \begin{array}{c} \diagup \diagdown \\ \diagdown \diagup \end{array} \text{N}^{2-}$	565	3.22		
$\text{Ru}(\text{NH}_3)_5 \text{N} \begin{array}{c} \diagup \diagdown \\ \diagdown \diagup \end{array} \text{NH} \begin{array}{c} \diagup \diagdown \\ \diagdown \diagup \end{array} \text{N}^{2+}$	416 (424 <sup>b</sup> )	11.1 (12.0)		1275
$\text{Ru}(\text{NH}_3)_5 \text{N} \begin{array}{c} \diagup \diagdown \\ \diagdown \diagup \end{array} \text{NH} \begin{array}{c} \diagup \diagdown \\ \diagdown \diagup \end{array} \text{N}^{3+}$	519 (511 <sup>b</sup> )	3.73 (3.63)		1350
$(\text{CN})_5\text{Fe} \text{N} \begin{array}{c} \diagup \diagdown \\ \diagdown \diagup \end{array} \text{NH} \begin{array}{c} \diagup \diagdown \\ \diagdown \diagup \end{array} \text{NRu}(\text{NH}_3)_5^-$	377(sh)	11.0	2045	1280
	426	14.8		
$(\text{CN})_5\text{Fe} \text{N} \begin{array}{c} \diagup \diagdown \\ \diagdown \diagup \end{array} \text{NH} \begin{array}{c} \diagup \diagdown \\ \diagdown \diagup \end{array} \text{NRu}(\text{NH}_3)_5$	400	9.89	2041	1351
	506	4.56		
$(\text{CN})_5\text{Fe} \text{N} \begin{array}{c} \diagup \diagdown \\ \diagdown \diagup \end{array} \text{NH} \begin{array}{c} \diagup \diagdown \\ \diagdown \diagup \end{array} \text{NRu}(\text{NH}_3)_5^+$	344	9.86	2125	1330
	522	3.84		

<sup>a</sup> UV-vis spectra are measured in solution at pH = 8 (tris). IR spectra are measured in solid as a KBr pellet. <sup>b</sup> Reference 8.

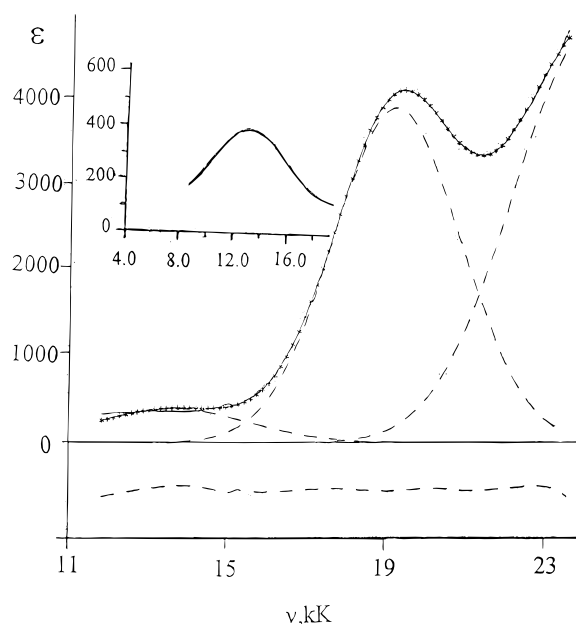
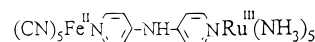
**Table 2.** Reduction Potentials of  $\text{Fe}(\text{CN})_5\text{L}^{2-/3-}$  and  $\text{Ru}(\text{NH}_3)_5\text{L}^{3+/2+}$  Complexes<sup>a</sup>

Complex	$E_{1/2}$ , V vs NHE
$\text{Fe}(\text{CN})_5 \text{N} \begin{array}{c} \diagup \diagdown \\ \diagdown \diagup \end{array} \text{NH} \begin{array}{c} \diagup \diagdown \\ \diagdown \diagup \end{array} \text{N}^{2-/3-}$	0.40
$\text{Ru}(\text{NH}_3)_5 \text{N} \begin{array}{c} \diagup \diagdown \\ \diagdown \diagup \end{array} \text{NH} \begin{array}{c} \diagup \diagdown \\ \diagdown \diagup \end{array} \text{N}^{3+/2+}$	0.22
$\text{Ru}(\text{NH}_3)_5 \text{N} \begin{array}{c} \diagup \diagdown \\ \diagdown \diagup \end{array} \text{NH} \begin{array}{c} \diagup \diagdown \\ \diagdown \diagup \end{array} \text{NH}^{4+/3+}$	0.29 <sup>b</sup>
$(\text{CN})_5\text{Fe} \text{N} \begin{array}{c} \diagup \diagdown \\ \diagdown \diagup \end{array} \text{NH} \begin{array}{c} \diagup \diagdown \\ \diagdown \diagup \end{array} \text{NRu}(\text{NH}_3)_5^{0/1-}$	0.17
$(\text{CN})_5\text{Fe} \text{N} \begin{array}{c} \diagup \diagdown \\ \diagdown \diagup \end{array} \text{NH} \begin{array}{c} \diagup \diagdown \\ \diagdown \diagup \end{array} \text{NRu}(\text{NH}_3)_5^{1+/0}$	0.44

<sup>a</sup>  $\mu = 0.10$  M LiClO<sub>4</sub>, pH = 8 (tris), unless otherwise specified.  
<sup>b</sup> Measured in 0.10 M HClO<sub>4</sub>.

complexes and the corresponding mononuclear complexes are summarized in Table 1. As compared with the spectra of the mononuclear complexes, two band maxima at 400 and 506 nm for the mixed valence molecule can be interpreted as due to the MLCT of Fe(II) and LMCT of Ru(III), respectively. Infrared spectra and electrochemical results also agree with the above assignment. The characteristic infrared bands are also listed in Table 1. The cyanide stretching frequency of 2041 cm<sup>-1</sup> and the frequency for the symmetric ammonia deformation mode at 1351 cm<sup>-1</sup> clearly indicate that the mixed valence species belongs to Fe(II) and Ru(III) valence-trapped localized system.<sup>15,16</sup> The reduction potentials of the mono- and binuclear complexes under study are listed in Table 2. As shown from the table, the first step oxidation of  $(\text{CN})_5\text{Fe}(\text{pyNHpy})\text{Ru}(\text{NH}_3)_5^-$  at  $E_{1/2} = 0.17$  V suggests that the oxidation goes to  $\text{Ru}(\text{NH}_3)_5^{2+}$  center. Furthermore, the second-step oxidation with  $E_{1/2} = 0.44$  V is similar to that of the  $\text{Fe}(\text{CN})_5\text{pyNHpy}^{2-/3-}$  couple.

The UV-vis spectrum of the **M** showed a bump in the 600–900 nm region which is absent for both **R** and **O**. Obviously, this arises from the contribution of the intervalence band which is buried in the LMCT absorption of the mixed valence species. By analyzing the absorption between 430–900 nm with the deconvolution method using CURFIT program,<sup>17</sup> we were able

**Figure 1.** Deconvolution Analysis of Absorption Spectrum of

to resolve the IT band as shown in Figure 1. The band has a  $\lambda_{\max} = 725$  nm ( $\epsilon_{\max} = 600$  M<sup>-1</sup> cm<sup>-1</sup>) and  $\Delta\bar{\nu}_{1/2} = 5.4 \times 10^3$  cm<sup>-1</sup>. The analysis of the IT band according to Hush's theory<sup>18</sup> yields values of  $\Delta\bar{\nu}_{1/2(\text{calc})}$ ,  $\alpha^2$ , and  $H_{\text{AB}}$  as  $5.4 \times 10^3$  cm<sup>-1</sup>,  $1.3 \times 10^{-3}$ , and  $5.0 \times 10^2$  cm<sup>-1</sup>, respectively.

**Kinetics of Substitution and Oxidation Reactions of Binuclear Complexes.** The specific rate constants of formation of  $\text{Fe}(\text{CN})_5\text{L}^{3-}$  (L = pyNHpy,  $\text{Ru}(\text{NH}_3)_5\text{pyNHpy}^{2+}$ , and  $\text{Ru}(\text{NH}_3)_5\text{pyNHpy}^{3+}$ ) complexes according to eq 1 are listed in column 2 of Table 3. Due to the interference of the outer-sphere redox reaction<sup>1</sup> between  $\text{Fe}(\text{CN})_5\text{OH}_2^{3-}$  ( $E_{1/2} = 0.39$  V<sup>19</sup>) and

(15) Dows, D. A.; Wilmarth, W. K.; Haim, A. *J. Inorg. Nucl. Chem.* **1961**, *21*, 33.

(16) Yeh, A.; Haim, A.; Tanner, M.; Ludi, A. *Inorg. Chim. Acta* **1979**, *33*, 51.

(17) Wang, S. L.; Wang, P. C.; Nieh, Y. P. *J. Appl. Crystallogr.* **1990**, *23*, 520.

(18) Hush, N. S. *Prog. Inorg. Chem.* **1967**, *8*, 391.

(19) Toma, H. E.; Creutz, C. *Inorg. Chem.* **1977**, *16*, 545.

(20) Fürholz, U.; Haim, A. *Inorg. Chem.* **1987**, *26*, 3243.

(21) Richardson, D. E.; Taube, H. *J. Am. Chem. Soc.* **1983**, *105*, 40.

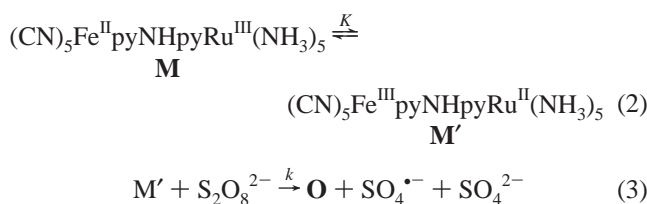
**Table 3.** Rate Constants of Formation and Dissociation of Pentacyanoferrate(II)

L	$10^{-2} k_f, \text{M}^{-1}\text{s}^{-1}$	$10^3 k_d, \text{s}^{-1}$	$10^5 K, \text{M}^{-1}$
	1.64±0.03	0.732±0.009	2.24
Ru(NH <sub>3</sub> ) <sub>5</sub> N	15.3±0.4	2.33±0.01	6.57
Ru(NH <sub>3</sub> ) <sub>5</sub> N	34.5±0.9	1.27±0.06	27.2

<sup>a</sup>  $\mu = 0.10 \text{ M LiClO}_4$ , pH = 8 (tris),  $T = 25 \text{ }^\circ\text{C}$ .

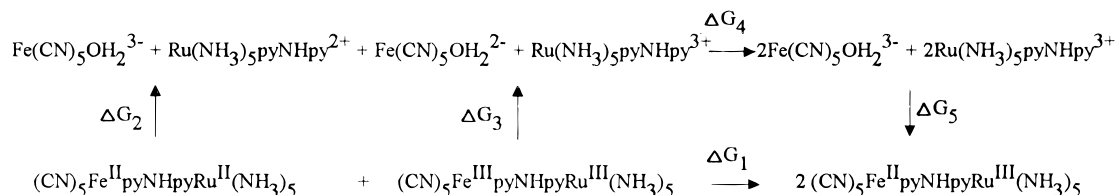
Ru(NH<sub>3</sub>)<sub>5</sub>pyNHpy<sup>3+</sup>, the  $k_f$  for the mixed valence molecule has been corrected for the stoichiometry of Fe(CN)<sub>5</sub>OH<sub>2</sub><sup>3-</sup> concentration. The rate constants of dissociation were also measured and the results were expressed in column 3 of Table 3. The equilibrium constants as obtained from  $k_f/k_d$  are also listed in Table 3. The equilibrium constant for the formation of **M** of  $2.7 \times 10^6 \text{ M}^{-1}$  agrees reasonably well with that obtained from the electrochemical data and the equilibrium quotient for the formation of the **R**,<sup>19</sup> which has a value of  $4.6 \times 10^6 \text{ M}^{-1}$ .

The second-order rate constants of oxidation for the complexes under study are listed in Table 4. The oxidation of **R**, as observed by the absorbance decrease at 426 nm, is biphasic which corresponds to two separate stages of oxidation, namely from **R** to **M** and **M** to **O**. Due to the large rate difference, the rate of each step can be measured separately without interfering with each other. The rate constant of the first stage oxidation agrees well with that of the oxidation of Ru(NH<sub>3</sub>)<sub>5</sub>pyNHpy<sup>2+</sup> complex, implying that the oxidation goes to the Ru(II) site. The rate constant of oxidation of **M** which agrees within experimental error with that of the second phase of oxidation of **R**, has a value of  $16.9 \text{ M}^{-1} \text{ s}^{-1}$ . This is greater than that of the oxidation of Fe(CN)<sub>5</sub>pyNHpy<sup>3-</sup> complex by ~2 orders of magnitude, inferring that the direct oxidation of the Fe(II) center is not likely. Instead, we tend to favor that the oxidation proceeds via rapid and reversible isomerization of **M** to its oxidation state isomer **M'** (eq 2), which is followed by the reaction of **M'** with S<sub>2</sub>O<sub>8</sub><sup>2-</sup> to **O**, as proposed previously.<sup>3,5,6</sup>



According to this mechanism,  $k_{\text{ox}} = kK$ . The reduction potential for the O/M' couple can be approximated by the reduction potential of the Ru(NH<sub>3</sub>)<sub>5</sub>pyNHpyH<sup>4+/3+</sup> couple due to the small coupling between metal centers of the binuclear complex. Thus, the value of  $K$ , as obtained from the electrochemical data, is  $2 \times 10^{-3}$ . Therefore,  $k = 5.8 \times 10^3 \text{ M}^{-1} \text{ s}^{-1}$ , as is expected for the oxidation of a Ru(II) center.<sup>20</sup>

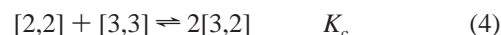
### Scheme 1

**Table 4.** Specific Rate Constants of Oxidation of Fe(II) and Ru(II) Complexes<sup>a</sup>

Complex	$k_{\text{ox}}^b, \text{M}^{-1}\text{s}^{-1}$
Fe(CN) <sub>5</sub> N	0.414±0.008
Ru(NH <sub>3</sub> ) <sub>5</sub> N	(2.41±0.06)×10 <sup>4</sup>
(CN) <sub>5</sub> Fe N	(3.54±0.09)×10 <sup>4</sup>
CN) <sub>5</sub> Fe N	16.9±0.3

<sup>a</sup>  $\mu = 0.10 \text{ M LiClO}_4$ , pH = 8 (tris),  $T = 25 \text{ }^\circ\text{C}$ . <sup>b</sup>  $k_{\text{ox}} = k_{\text{obs}}/2[\text{S}_2\text{O}_8^{2-}]$ .

**Stability of Binuclear Complexes.** The comproportionation constant for eq 4, as calculated from the appropriate reduction potentials, is  $3.9 \times 10^4$ .



This corresponds to  $3.2 \text{ kcal mol}^{-1}$  additional stability of **M** with respect to its isoivalent states. The stability associated with the interaction between metal centers ( $\alpha^2\nu_{\text{max}}$ )<sup>21</sup> is  $0.05 \text{ kcal mol}^{-1}$ . This contribution of resonance stability energy is almost negligible, as expected since the system is best described as featuring trapped-valence states. Moreover, the bridge ligand may not adopt a planar configuration in order to avoid the steric hindrance, and this will make the communication between metal centers even more difficult. The MP2/STO-3G and MP2/6-31+G ab initio calculations both indicate that the pyridine rings in the dipyridylamine are tilted with an angle of  $\sim 50^\circ$ . The electrostatic factor, as calculated from the ion pair formation constants,<sup>20</sup> also yields only  $0.8 \text{ kcal mol}^{-1}$  in favor of the stability of the mixed valence species. In order to account for another  $2.3 \text{ kcal mol}^{-1}$  extra stability of **M** still left, we will consider the thermodynamic cycle in Scheme 1.<sup>1</sup>

Values of  $\Delta G_1$ ,  $\Delta G_2$ ,  $\Delta G_3$ ,  $\Delta G_4$ , and  $\Delta G_5$  as calculated from the equilibrium constants and the reduction potentials are  $-6.2$ ,  $7.9$ ,  $7.6$ ,  $-3.9$ , and  $-17.6 \text{ kcal}$ , respectively. Apparently, the difference in the intrinsic relative stability of Fe<sup>II</sup>/Fe<sup>III</sup> vs Ru<sup>II</sup>/Ru<sup>III</sup> ( $\Delta G_4$ ) is attributed to the stability of **M**. Furthermore, this relative intrinsic stability also accounts for the stability of **M** with respect to its electronic isomer **M'**. The free energy change between the two isomers, calculated from the equilibrium constant of eq 2, is  $3.5 \text{ kcal}$ . The electrostatic contribution ( $3+,3-$  vs  $2+,2-$  moieties) only amounts to  $1.4 \text{ kcal mol}^{-1}$  in favor of **M**. However, the relative stability factor favors **M** by  $3.9 \text{ kcal}$ .

The comproportionation constant for the binuclear complexes of diruthenium analog is  $26$ ,<sup>8</sup> three orders of magnitude smaller than that of our present system. The contributions of both the charge effect ( $0.14 \text{ kcal}$ ) and the resonance ( $0.07 \text{ kcal}$ ) of the mixed valence ion are not significantly different from those of the Fe<sup>II</sup>-Ru<sup>III</sup> binuclear complex. Evidently, the small  $K_c$  value

for the diruthenium binuclear complexes arises from the lack of the equilibrium barrier between the oxidation state electronic isomers of the mixed valence ion. For symmetric homonuclear mixed valence compounds, there is no difference in energy between **M** and **M'**.

In the pyrazine bridged binuclear complexes,<sup>1</sup> it was found that the predominant factor for the stability of the mixed valence species resided mainly in the contrasting affinities of **M** with respect to that of **R** and **O** (4.2 kcal mol<sup>-1</sup>), which is a result of strong  $d\pi \rightarrow \pi_L^*$  backbonding of the mixed valence compound. However, in our present system, this factor contributes only 1.1 kcal mol<sup>-1</sup> in favor of **M**. This small contribution may not arise from the lack of MLCT stabilization of **M**. Rather, it may be due to the  $\pi_L$  to M(III) stabilization of the oxidized form which apparently is absent in the pyrazine bridged complexes. It is noteworthy that the affinity of (CN)<sub>5</sub>Fe<sup>III</sup>pyNHpyRu<sup>III</sup>-(NH<sub>3</sub>)<sub>5</sub> is  $3.9 \times 10^5$  M<sup>-1</sup> as compared to that of 41 M<sup>-1</sup> for the

(CN)<sub>5</sub>Fe<sup>III</sup>pzRu<sup>III</sup>(NH<sub>3</sub>)<sub>5</sub>.<sup>1</sup> Obviously, the difference in stability as high as 5.5 kcal comes from the LMCT stabilization of the dipyriddyamine-bridged species.

**Acknowledgment.** The support of this work by the National Science Council of the Republic of China under Grant NSC 86-2113-M-029-004 is gratefully acknowledged. We also thank Professor Hsiu-Yao Cheng for the assistance in the theoretical calculations.

**Supporting Information Available:** Table S1 listing pseudo-first-order rate constants for the formation of Fe(CN)<sub>5</sub>L<sup>3-</sup> complexes; Table S2 listing pseudo-first-order rate constants for the oxidation of Fe(II) and Ru(II) complexes; Figure S1 containing absorption spectra of binuclear complexes; and Figure S2 containing a cyclic voltammogram of (CN)<sub>5</sub>FepyNHpyRu(NH<sub>3</sub>)<sub>5</sub><sup>-</sup>. This material is available free of charge via the Internet at <http://pubs.acs.org>.

IC980087D